

Available online at www.sciencedirect.com

ScienceDirect

www.elsevier.com/locate/jes

JES
JOURNAL OF
ENVIRONMENTAL
SCIENCES
www.jesc.ac.cn

Effect of drainage on CO₂, CH₄, and N₂O fluxes from aquaculture ponds during winter in a subtropical estuary of China

Ping Yang^{1,3}, Derrick Y.F. Lai², Jia F. Huang^{1,3}, Chuan Tong^{1,3,*}

1. School of Geographical Sciences, Fujian Normal University, Fuzhou 350007, China. E-mail: yangping528@sina.cn

2. Department of Geography and Resource Management, and Centre for Environmental Policy and Resource Management, The Chinese University of Hong Kong, Shatin, New Territories, Hong Kong, China

3. Key Laboratory of Humid Sub-tropical Eco-geographical Process of Ministry of Education of China, Fujian Normal University, Fuzhou 350007, China

ARTICLE INFO

Article history:

Received 23 September 2016

Revised 28 December 2016

Available online 30 March 2017

Keywords:

Aquaculture pond

Drainage management

Greenhouse gas flux

Global warming

Min River estuary

ABSTRACT

Aquaculture ponds are dominant features of the landscape in the coastal zone of China. Generally, aquaculture ponds are drained during the non-culture period in winter. However, the effects of such drainage on the production and flux of greenhouse gases (GHGs) from aquaculture ponds are largely unknown. In the present study, field-based research was performed to compare the GHG fluxes between one drained pond (DP, with a water depth of 0.05 m) and one undrained pond (UDP, with a water depth of 1.16 m) during one winter in the Min River estuary of southeast China. Over the entire study period, the mean CO₂ flux in the DP was (0.75 ± 0.12) mmol/(m²·hr), which was significantly higher than that in the UDP of (-0.49 ± 0.09) mmol/(m²·hr) ($p < 0.01$). This indicates that drainage drastically transforms aquaculture ponds from a net sink to a net source of CO₂ in winter. Mean CH₄ and N₂O emissions were significantly higher in the DP compared to those in the UDP (CH₄ = (0.66 ± 0.31) vs. (0.07 ± 0.06) mmol/(m²·hr) and N₂O = (19.54 ± 2.08) vs. (0.01 ± 0.04) μmol/(m²·hr)) ($p < 0.01$), suggesting that drainage would also significantly enhance CH₄ and N₂O emissions. Changes in environmental variables (including sediment temperature, pH, salinity, redox status, and water depth) contributed significantly to the enhanced GHG emissions following pond drainage. Furthermore, analysis of the sustained-flux global warming and cooling potentials indicated that the combined global warming potentials of the GHG fluxes were significantly higher in the DP than in the UDP ($p < 0.01$), with values of 739.18 and 26.46 mgCO₂-eq/(m²·hr), respectively. Our findings suggested that drainage of aquaculture ponds can increase the emissions of potent GHGs from the coastal zone of China to the atmosphere during winter, further aggravating the problem of global warming.

© 2017 The Research Center for Eco-Environmental Sciences, Chinese Academy of Sciences.

Published by Elsevier B.V.

Introduction

The global supply of fishery food products has increased dramatically over the last five decades, with an average

growth rate of 3.2% per year during 1961–2009, as a response to the rising global demand for proteins (Hu et al., 2014). As production by capture fisheries has leveled off since the 1970s, the aquaculture industry will play a significant role in

* Corresponding author. E-mail: tongch@fjnu.edu.cn (Chuan Tong).

meeting the increasing demand for aquatic foods (e.g., fish and shellfish) (Hu et al., 2012). As one of the main components of the aquaculture system, aquaculture ponds are widely distributed around the world (FAO, 2014). At present, the combined surface area of freshwater and brackish aquaculture ponds is estimated to be 110,832 km² globally (Verdegem and Bosma, 2009). Although these aquaculture ponds are very effective in responding to the ever-growing global demand for fishery-produced food products, the rapid development of aquaculture also has led to serious environmental concerns (Hu et al., 2012; Paudel et al., 2015). One of the major environmental concerns is associated with climate change via the release of greenhouse gases (GHGs) from aquaculture ponds (Williams and Crutzen, 2010; Hu et al., 2014).

Numerous previous studies have suggested that high GHG production and emissions from natural aquatic ecosystems (e.g., lakes, river, streams, and estuary) are dependent on a large supply of organic matter (Repo et al., 2007; Clough et al., 2011; Yang et al., 2015; Schade et al., 2016). Aquaculture ponds are semi-artificial ecosystems, which maintain a high supply level of organic matter through phytoplankton feeding and photosynthesis. Given the rather low feed utilization efficiency of aquatic animals (e.g., fish, shrimp, and crab) (Avnimelech and Ritvo, 2003; Su et al., 2009), these ponds generally retain a large quantity of organic matter from residual feed and feces (Chen et al., 2016). Consequently, high GHG emissions from aquaculture ponds have been observed in some studies during the culture period (Datta et al., 2009; Chen et al., 2015, 2016). However, few studies to date have focused on the effects of drainage on GHG emissions and its controlling factors in aquaculture ponds during the non-culture period.

The bottom of an aquaculture pond is the main habitat for aquatic animals and its environment is closely associated with the healthy growth of aquatic animals (Zeng et al., 2013). Annual drainage is a typical management activity practiced by the operators as a way to export aquaculture effluent, accelerate aerobic decomposition of bottom soils, and avoid eutrophication during the non-culture period after harvest (Molnar et al., 2013; Herbeck et al., 2013; Hu et al., 2016). Drainage activities can cause large changes in hydrology, nutrient cycling, sediment physicochemical properties, and even broad ecosystem functions (Dinsmore et al., 2009; Haque et al., 2016). The effects of drainage on GHG emissions have been reported for peatland and paddy fields. The general consensus from previous studies is that drainage increases atmospheric oxygen diffusion into soils, thereby enhancing aerobic decomposition and promoting CO₂ and N₂O emissions, while at the same time reducing CH₄ emissions (Yagi et al., 1996; Dinsmore et al., 2009; Hatala et al., 2012; Pandey et al., 2014; Haque et al., 2016). Therefore, the variation and magnitude of GHG emissions are expected to differ significantly between undrained and drained aquaculture ponds, but this has not been experimentally verified.

Asia accounts for approximately 90% of the world's aquaculture production (FAO, 2012), and China is a leading producer of aquaculture products (The Fishery Bureau, Ministry of Agriculture of PRC, 2014). According to statistical data maintained by Verdegem and Bosma (2009), the combined water surface area of aquaculture ponds in China is estimated to be 58,579 km². The aquaculture ponds in the Fujian Province in southeast China are

typically operated for approximately eight to nine months of the year, followed by a short, non-culture period in winter. During the winter period, water in most of the ponds is drained for various reasons (e.g., to discharge polluted aquacultural sewage), directly exposing the unconsumed bait feed and biological residues from the previous culture period to the atmosphere. These residues provide an abundant supply of labile carbon and nitrogen to microbes that can stimulate microbial decomposition and subsequent GHG emissions. Yet, the potential contribution of GHG fluxes to radiative forcing from the drained aquaculture ponds during winter months remains poorly documented. This oversight could possibly lead to a biased estimate of the contribution of aquaculture ponds to radiative forcing and future climate change. Hence, in this study, we aim to fill this knowledge gap by comparing the magnitude, temporal variations, and environmental controls of GHG fluxes between a regularly drained aquaculture pond and an undrained aquaculture pond in a subtropical estuary in China.

1. Material and methods

1.1. Study site description

This study was carried out in the Shanyutan Nature Reserve (26°00'36"N–26°03'42"N, 119°34'12"E–119°40'40"E) (Fig. 1), in the Min River estuary of southeast China. The nature reserve has a surface area totaling approximately 31.2 km². The area has a subtropical monsoonal climate, with mean annual temperature and rainfall of 19.6°C and 1350 mm, respectively (Tong et al., 2013). Salt water pumped from the coastal sea and locally drawn fresh water are used in the aquaculture ponds. The two main types of aquaculture ponds are shrimp and polyculture (fish and shrimp) ponds. During the non-culture period in winter, pond operators in this area usually drain the ponds, with the duration of drainage varying between the ponds. In most of the polyculture ponds, the drainage period lasts from December to March. In this study, we selected one drained polyculture pond (DP) and one undrained polyculture pond (UDP) for comparison of their GHG fluxes during winter. There was no significant difference in the physicochemical properties of the sediment and water in the two ponds during the aquaculture period (from June to November) based on previous investigations at these sites. The distance between the DP and UDP is approximately 150 m (Fig. 1). The surface areas of the UDP and the DP were approximately 1100 and 1200 m², respectively, and the mean water depth over the study period was 1.2 m in the UDP and 0.05 m in the DP. During the culture period, the breeding densities of prawns and grass carp were 35 prawn/m² and 5 carp/m², respectively. Feed (Yuehai™, Guangzhou, China) was applied to the ponds three times daily at 07:00, 11:00, and 17:00. The feeding rate was maintained around 20–60 kg/day during the culture period, and the amount of feed applied was determined based on the animal response to the previous feeding.

1.2. Gas sampling and flux estimation

CO₂, CH₄, and N₂O fluxes from the UDP were measured using floating static chambers, similar to those described by

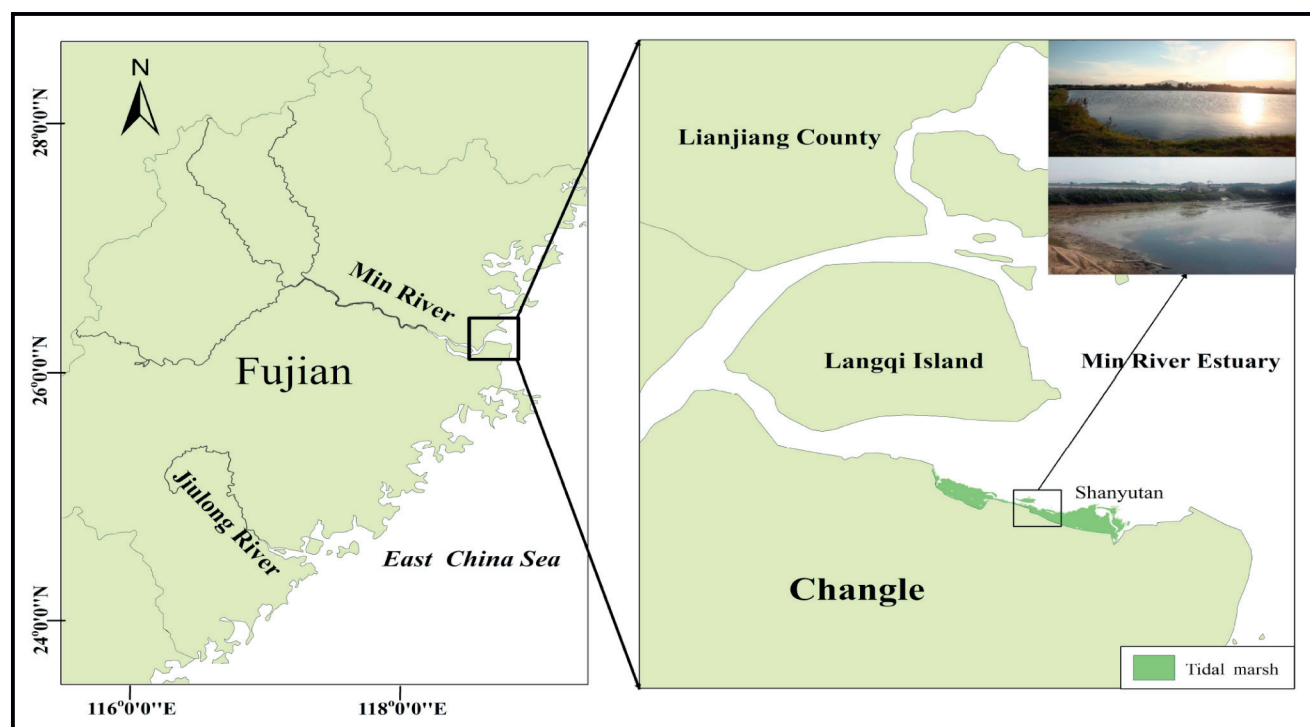


Fig. 1 – Location of the study area and measurement sites in the Shanyutan wetland of the Min River estuary.

Bastviken et al. (2010), Diem et al. (2012), and Zhao et al. (2013). The floating chambers consisted of two parts: a floating bottom collar and an open-bottomed chamber made of transparent Plexiglas® (inner diameter 38.5 cm × height 45 cm). The gas samples were collected by boat at the center of the ponds. CO₂, CH₄, and N₂O fluxes from the DP were measured using enclosed static chambers (Tong et al., 2013). The enclosed static chamber also consisted of two parts: a stainless steel bottom collar (35 × 35 cm; 30 cm in depth) and a chamber made of transparent Plexiglas® (35 × 35 cm; 60 cm in height). The bottom collar was inserted into the pond sediment to a depth of 30 cm one week before the flux measurements. To minimize possible disturbances of the measurement sites during sampling, a wooden boardwalk was built for accessing the DP sites. Four replicate chambers, each separated by a distance of approximately 0.5 m, were deployed in each pond for the flux measurements.

Sampling campaigns at the UDP and the DP were undertaken at an interval of 7 to 10 days between December 10, 2011 and January 20, 2012, with a total of six campaigns. Each measurement campaign involved the deployment of 8 chambers in two ponds (four chambers per pond). On each sampling day, we measured GHG fluxes twice, at 09:00–10:00 and 15:00–16:00 (China Standard Time), respectively. The headspace gas samples were collected by syringe and transferred to pre-evacuated airtight gas sampling bags (50 mL) at 15 min intervals over a 45 min period after chamber enclosure, i.e., four gas samples were obtained. CO₂ concentrations were determined using a gas chromatograph (GC-2014, Shimadzu, Kyoto, Japan) equipped with a thermal conductivity detector (TCD). The CH₄ and N₂O concentrations were determined using a gas chromatograph (GC-2014,

Shimadzu, Kyoto, Japan) equipped with a pulsed discharge detector (PDD). The gas chromatography configurations for analyzing CO₂, CH₄, and N₂O concentrations followed the same method as described in Tong et al. (2013).

The CO₂, CH₄, and N₂O concentrations were determined using the ideal gas law, along with supporting data such as air temperature, atmospheric pressure, and molar mass of the gas species concerned (Yang et al., 2013; Tangen et al., 2016). The flux rates for CO₂, CH₄ (mmol/(m²·hr)), and N₂O (μmol/(m²·hr)) were then determined from linear regression of the gas concentrations against time (Gleason et al., 2009; Tangen et al., 2016).

For decades, global warming potential (GWP) has been applied to evaluate the effect of GHG emissions of an individual system on the radiative forcing of the climate. Neubauer and Megonigal (2015) emphasize the limited applicability of the GWP for the calculation of GHG balances, due to the basic assumption that emissions occur as a single pulse (Witte and Giani, 2016). Hence, sustained-flux global warming potentials (SGWPs) for gas emissions and sustained-flux global cooling potentials (SGCPs) for gas uptakes were calculated in CO₂ equivalents using the 100-year time frame values presented by Neubauer and Megonigal (2015). In this study, the SGWP/SGCP calculations were performed following the descriptions in Neubauer and Megonigal (2015) and Tangen et al. (2016).

1.3. Ancillary environmental measurements

During each sampling campaign, we measured sediment pH, redox potential (E_h), and salinity indicated by conductivity (EC) (Tamn and Wong, 1998). Sediment temperature, pH, and

E_h at a depth of 10 cm were determined *in situ* using an IQ150 instrument (IQ Scientific Instruments, Carlsbad, CA, USA). The EC at a depth of 10 cm was measured *in situ* by a 2265FS EC Meter (Spectrum Technologies Inc., USA). On each sampling day, water samples were collected at a depth of 0.1 m from the UDP, with four replicates for SO_4^{2-} and Chl-*a* (Chlorophyll *a*) analysis. Water samples were analyzed for SO_4^{2-} by ion chromatography (Dionex 2100, American) after being filtered through Whatman GF/F-filters. Chl-*a* was extracted with acetone (90%) in darkness for 24 hr after filtration of the water samples through GF/F glass microfiber filters and analyzed using an ultraviolet and visible spectrophotometer (UV–visible) spectrophotometer (Shimadzu UV-2450, Japan). Surface water samples from the DP were also collected for SO_4^{2-} and Chl-*a* analysis during the initial period of drainage (from 08 December to 26 December, 2011).

1.4. Data analysis

We tested for significant differences in GHG (CO_2 , CH_4 , and N_2O) fluxes between UDP and DP during the study period using the repeated measures analysis of variance (RMANOVA). RMANOVA was also used to examine differences between the UDP and DP in temperature, pH, E_h , and EC of the sediments. The independent-sample t-test was used to examine differences in the SO_4^{2-} and Chl-*a* concentrations of the water and in the water depth between the UDP and DP. Correlations between the environmental variables and the GHG fluxes were tested with the Pearson correlation analysis. All statistical analyses were carried out using SPSS version 17.0 (SPSS, Inc., USA) and Microsoft Excel. Statistical results with $p < 0.05$ were considered significant.

2. Results

2.1. Surface sediment/water physicochemical parameters in aquaculture ponds

The mean values obtained for several surface sediment and water physicochemical parameters are shown in Table 1. The mean sediment temperature and E_h in the UDP were significantly lower than those in the DP, while the pH and EC were significantly higher. Surface water Chl-*a* concentrations in the UDP were also significantly higher than those in the DP.

The mean water depth showed a decreasing trend in both ponds during the winter period (Fig. 2), and was significantly higher in the UDP than it was in the DP (1.16 vs. 0.05 m, $p < 0.05$, $n = 48$). Temporal variations in the sediment and water physicochemical parameters in the UDP and DP are presented in Fig. 3. These environmental parameters (*e.g.*, temperature, EC, pH, and E_h) followed a similar temporal trend in both ponds (Fig. 3), but the sediment temperature, EC, and E_h were more variable over time in the DP than they were in the UDP (Fig. 3a, b, and d).

2.2. Effect of drainage on different GHG fluxes in aquaculture ponds

Temporal variations of CO_2 fluxes in the UDP and DP differed significantly over the observation period (Fig. 4). The net CO_2 fluxes in the UDP were negative over the observation period, with maximum and minimum fluxes occurring on January 20 (-0.62 mmol/(m²·hr)) and January 10 (-0.39 mmol/(m²·hr)) (Fig. 4a), respectively, indicating a net uptake of atmospheric CO_2 by the pond in winter. While net CO_2 fluxes in the DP were quite variable over the study period ranging from a net release of 2.65 mmol/(m²·hr) on December 18 to a net uptake of -0.49 mmol/(m²·hr) on January 20 (Fig. 4a). Overall, the DP acted as a net source of CO_2 in winter with a positive mean flux. Mean CO_2 fluxes were significantly higher in the DP than they were in the UDP (RMANOVA, $F_{1, 94} = 170.87$, $p < 0.01$) (Table 2).

CH_4 fluxes from the UDP and DP were relatively higher during the initial observation stage and then decreased gradually with time (Fig. 4b). Although the temporal patterns of CH_4 fluxes between the UDP and DP were very similar, the amplitude of the changes varied substantially (Fig. 4b). The CH_4 emission fluxes in the UDP and DP ranged from 0.003 to 0.31 mmol/(m²·hr) and 0.004 to 1.77 mmol/(m²·hr), respectively, with means of (0.07 ± 0.06) mmol/(m²·hr) and (0.66 ± 0.31) mmol/(m²·hr). Mean CH_4 emission fluxes in the DP were one order of magnitude higher than those in the UDP (RMANOVA, $F_{1, 94} = 29.74$, $p < 0.01$) (Table 2), indicating that the former was a strong CH_4 source in winter, while the latter was a weak source.

Temporal variations of the N_2O fluxes from the UDP and DP also showed significantly different patterns over the observation period (Fig. 4c). Two peaks from the DP were observed on December 18 and January 3, whereas only one peak was observed from the UDP. The N_2O flux was consistently low

Table 1 – Comparison of average sediment and water physicochemical properties* between the UDP and DP during the study period.

Type	Sediment physicochemical properties				Water physicochemical properties	
	Temperature (°C)	pH	E_h (mV)	EC (mS/cm)	SO_4^{2-} (mg/L)	Chl- <i>a</i> (μg/L)
UDP	10.10 ± 0.13a	9.35 ± 0.44a	−139.11 ± 3.79a	9.15 ± 0.07a	167.27 ± 4.7a	399.04 ± 21.75a
DP	11.50 ± 0.37b	7.22 ± 0.05b	−12.65 ± 3.02b	6.37 ± 0.24b	68.34 ± 4.85b	93.56 ± 3.09b

Statistically significant differences in sediment temperature, pH, E_h and EC between UDP and DP ($p < 0.05$) were calculated by using RMANOVA. Statistically significant differences SO_4^{2-} and Chl-*a* between UDP and DP ($p < 0.05$) were calculated by using independent-samples t-test and are indicated by different letters within each column.

UDP: undrained pond; DP: drained pond; RMANOVA: repeated measures analysis of variance.

* Values are means (±S.E.) of samples ($n = 48$ for sediment temperature, pH, E_h , and EC at depth of 10 cm; $n = 48$ for SO_4^{2-} and Chl-*a* at the surface water from UDP; $n = 24$ for SO_4^{2-} and Chl-*a* at the surface water from DP) collected from UDP and DP.

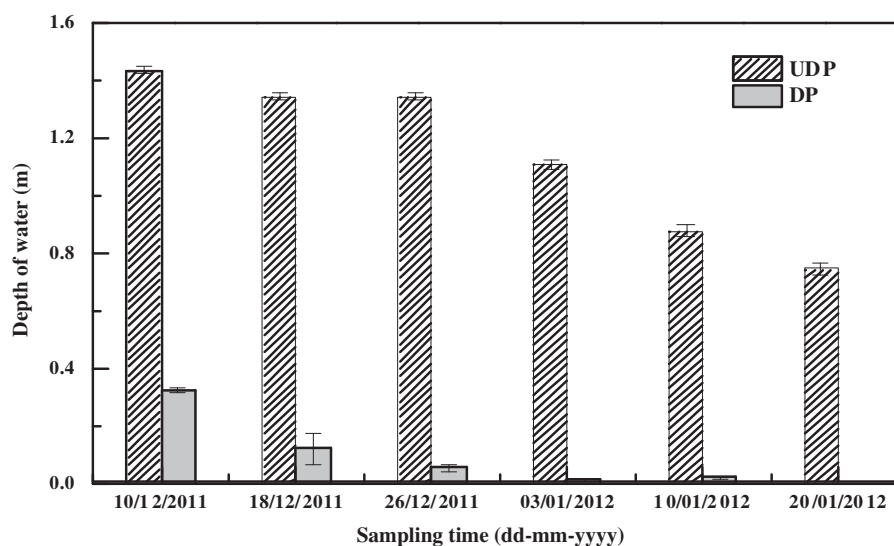


Fig. 2 – Variations in water depth in the UDP and DP from December 2011 to January 2012. Data points represent mean values \pm standard error ($n = 8$).

and quite variable in the UDP over the study period (Fig. 4c), ranging from a net release of $0.40 \mu\text{mol}/(\text{m}^2\cdot\text{hr})$ on December 10 to a net uptake of $-0.27 \mu\text{mol}/(\text{m}^2\cdot\text{hr})$ on January 10 (Table 2). In contrast with the UDP, the DP maintained high N_2O emissions over the study period (Fig. 4c), with fluxes ranging from 2.97 (January 20) to 36.07 (December 18) $\mu\text{mol}/(\text{m}^2\cdot\text{hr})$ (Table 2). The mean N_2O flux in the DP was $(19.54 \pm 2.08) \mu\text{mol}/(\text{m}^2\cdot\text{hr})$, which was significantly higher than that in the UDP of $0.01 \pm 0.04 \mu\text{mol}/(\text{m}^2\cdot\text{hr})$ (RMANOVA, $F_{1,94} = 164.07$, $p < 0.01$) (Table 2).

2.3. Effect of aquaculture pond drainage on SGWP/SGCP

The temporal pattern of CO_2 -eq fluxes from the UDP and DP differed greatly over the observation period, after taking into account the overall SGWP/SWCP values determined from all three GHGs (Fig. 5). CO_2 -eq fluxes in the UDP showed a decreasing trend with time, and CH_4 comprised the major contributor of the total calculated CO_2 -eq emissions. On the other hand, the CO_2 -eq fluxes in the DP initially increased, reaching a maximum on December 18, and then decreased gradually. In contrast with the UDP, CH_4 and N_2O contributed to the bulk of the overall CO_2 -eq emissions in the DP. In terms of overall SGWP/SGCP, the CO_2 -eq flux from the DP was $739.18 \text{ mgCO}_2\text{-eq}/(\text{m}^2\cdot\text{hr})$, which was approximately 27 times greater than that in the UDP of $26.46 \text{ mgCO}_2\text{-eq}/(\text{m}^2\cdot\text{hr})$ found for ($p < 0.01$), which indicated that the aquaculture ponds in southeast China's coastal zone make a substantial contribution to global warming during the non-aquaculture period (winter), which is a direct result of drainage.

2.4. Relationship between GHG fluxes and environmental factors

The relationships between GHG fluxes and environmental parameters are listed in Table 3. In the UDP, CO_2 fluxes had no significant correlations with any environmental parameters

except Chl-a ($p > 0.05$). On the other hand, CH_4 and N_2O fluxes showed significant, negative correlations with pH, EC, SO_4^{2-} , and Chl-a ($p < 0.01$), and significant, positive correlations with the water depth and E_h ($p < 0.01$) (Table 3). In the DP, sediment temperature was positively correlated with the fluxes of all three GHGs. CH_4 fluxes were significantly and negatively correlated with pH and SO_4^{2-} ($p < 0.01$), but positively correlated with water depth and E_h ($p < 0.01$) (Table 3). When data from the two ponds were combined, we found that fluxes of all three GHGs were positively correlated with sediment temperature and E_h ($p < 0.01$), but negatively correlated with water depth ($p < 0.001$), EC, and pH ($p < 0.01$, Table 3). Furthermore, CH_4 and N_2O fluxes showed significant negative correlations with SO_4^{2-} ($p < 0.01$), while CO_2 fluxes showed significant negative correlations with Chl-a ($p < 0.01$).

3. Discussion

3.1. Effect of aquaculture pond drainage on CO_2 fluxes

Over the study period, a consistent uptake (release) of CO_2 was observed in the UDP (DP), indicating that drainage during winter drastically transformed the aquaculture pond from a net CO_2 sink to a net source. This switch could possibly be attributed to the absence of flooding following the conversion of the flooded UDP to an exposed DP. In the present study, the UDP was continuously flooded over the observation period (Fig. 2) with a mean water depth of 1.2 m . The presence of an overlying water column could effectively reduce the diffusion of atmospheric oxygen into the sediment, thereby weakening the aerobic decomposition of organic matter and CO_2 production by aerobic microbes (Chimner and Cooper, 2003). In contrast, the DP was drained and the sediments were exposed to air for extended periods of time, which favored the decomposition of organic matter (e.g., unconsumed bait feed and biological residues) and microbial CO_2 production. This

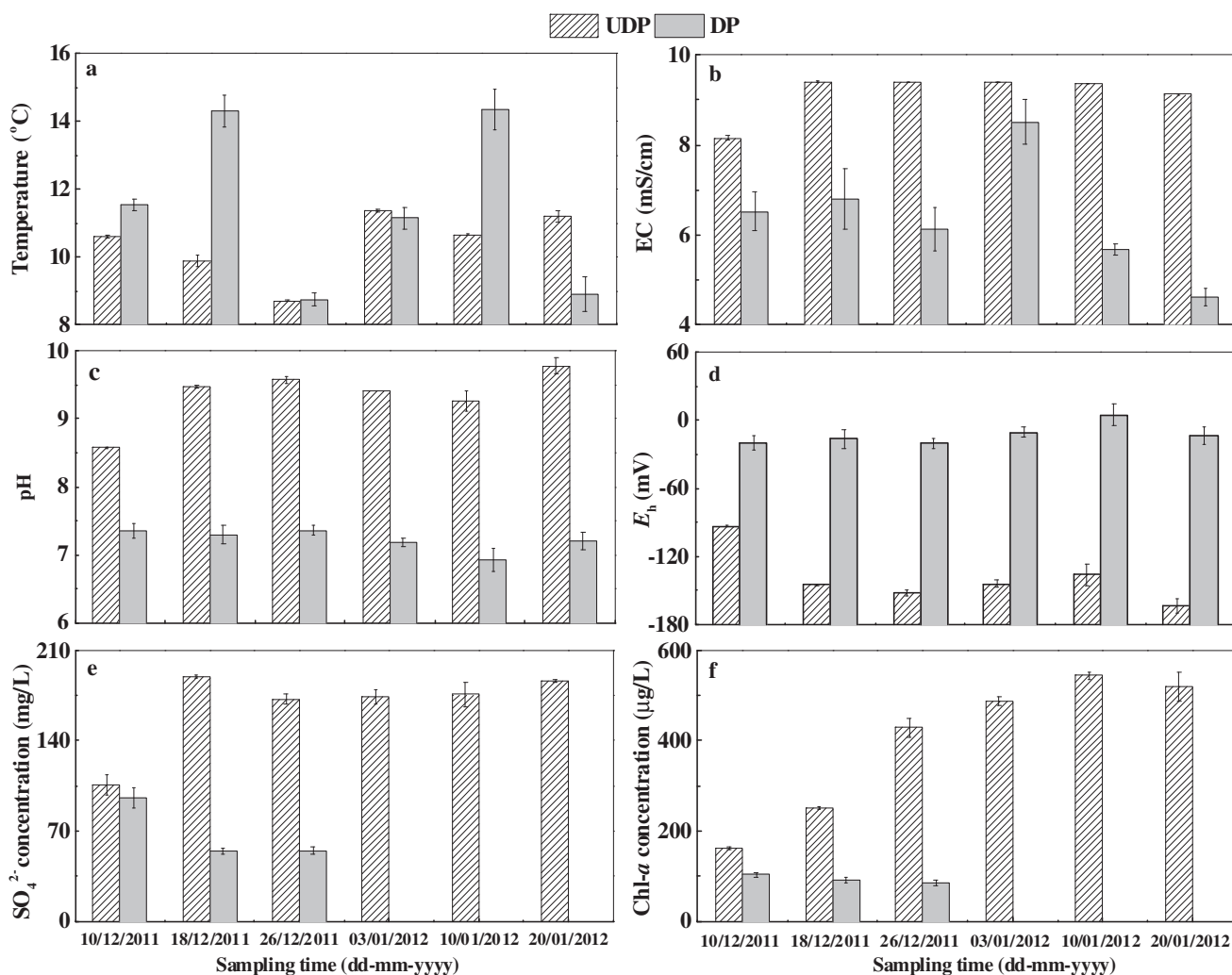


Fig. 3 – Variations in the sediment and water physicochemical parameters in the UDP and DP over the study period. Temperature, EC, pH, and E_h were measured in sediment from 0 to 10 cm depth, and SO_4^{2-} and Chl-*a* concentrations were measured in the surface water. Data points represent mean values \pm standard error ($n = 8$).

hypothesis was further supported by the strong correlations between water depth, sediment E_h , and CO_2 fluxes (Table 3).

Another effect of drainage that is also likely to influence CO_2 dynamics is the change in Chl-*a* concentrations. During the study period, we observed that the UDP had extremely high Chl-*a* concentrations (ranging from 162.44 to 520.41 $\mu g/L$) over the observation period (Fig. 3f), and net CO_2 uptake fluxes showed a significant, positive correlation with Chl-*a* (Table 3). These results showed that high photosynthesis rates arising from intensive phytoplankton blooms in the UDP could effectively sequester atmospheric CO_2 (Maberly, 1996; Gu et al., 2011; Wang et al., 2015). With the discharge of the aquaculture pond water, large quantities of phytoplankton are exported, which can eventually reduce the uptake of atmospheric CO_2 by photosynthesis.

Yet another drainage effect is the change in the salinity. A number of studies have indicated that high salinity inhibits organic carbon decomposition and mineralization processes, which reduces CO_2 production and emissions (Weston et al.,

2006; Chambers et al., 2013; Rath and Rousk, 2015). In this study, the mean salinity (represented by EC) in the UDP was (9.15 ± 0.04) mS/cm, which was significantly higher than that in the DP, at (6.37 ± 0.24) mS/cm (Table 1). The CO_2 fluxes from both ponds also showed a significant and negative relationship with salinity (Table 3), which lent support to the hypothesis that a decrease in salinity in DP might at least partly contribute to an increase in CO_2 emissions.

3.2. Effect of aquaculture pond drainage on CH_4 fluxes

CH_4 fluxes in the DP were considerably higher than those in the UDP over the observation period (Fig. 4b), which suggests that drainage could significantly promote CH_4 emissions from aquaculture ponds during the winter ($p < 0.01$, Table 2). One possible reason for the lower CH_4 emissions in the UDP is that a large proportion of the CH_4 produced from the sediment was oxidized in the overlying water column before it could reach the atmosphere via diffusive transport or ebullition. A

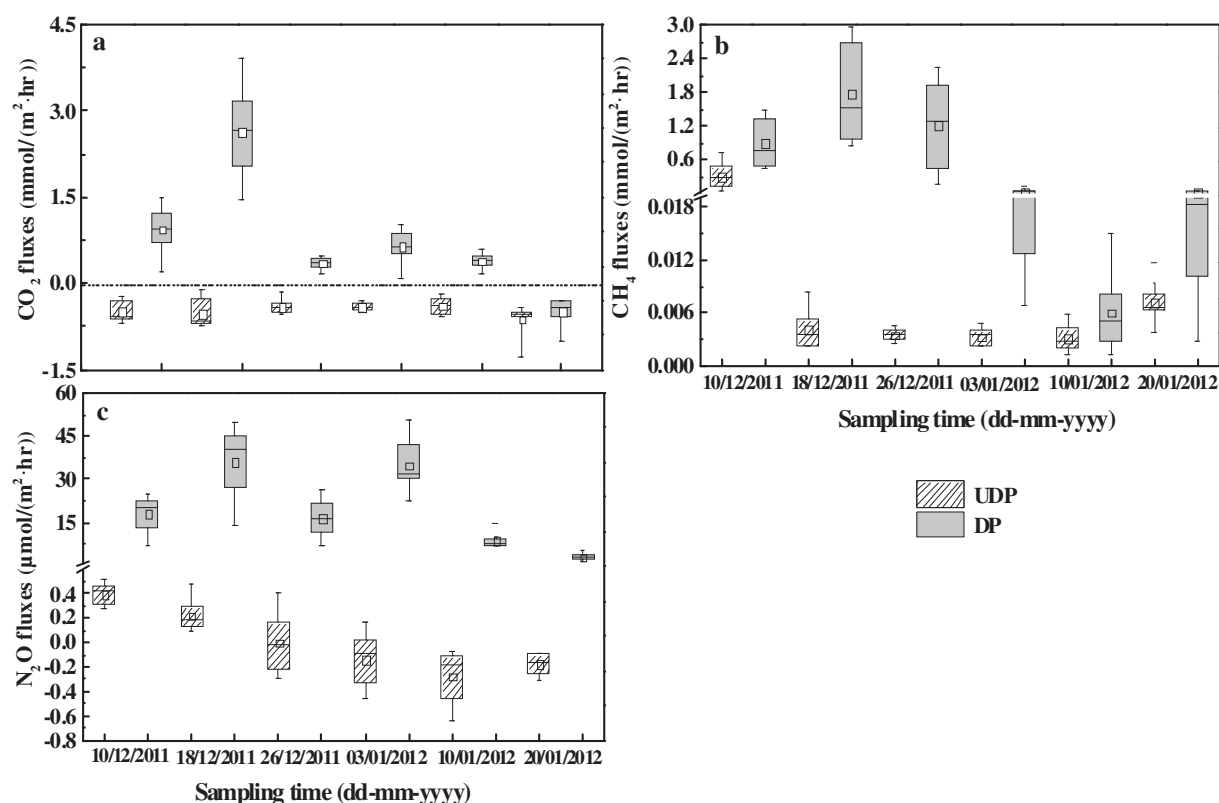


Fig. 4 – Fluxes of carbon dioxide (CO_2 , a), methane (CH_4 , b), and nitrous oxide (N_2O , c) from the UDP and DP during the study period. Boxes define the 25th and 75th percentiles, whiskers define the 5th and 95th percentiles, and center lines and squares show the median and mean values, respectively.

previous study showed that up to 80% of the CH_4 produced in deep sediments could be oxidized in the water column during the transport process (Bastviken et al., 2008). In contrast, the opportunity for CH_4 oxidation in the water column of the DP was much lower. Although the pond water was drained in winter (Fig. 2), the sediment retained a high level of moisture and a large amount of unconsumed feed and biological excreta during the initial period of drainage, which maintained a suitable environment for the microbial production of CH_4 .

Previous studies have shown that high pH and salinity could inhibit the activities of, or cause harm to, methanogens (Stow et al., 2005; Zeng et al., 2008; Clough et al., 2011), which

would subsequently reduce CH_4 production and emissions. In contrast, a near neutral environment and low salinity could enhance CH_4 emissions (Chen et al., 2010; Sun et al., 2013). In this study, the mean pH and salinity in the DP were significantly lower than those in the UDP, and the sediment pH in the DP was weakly alkaline (Table 1). Meanwhile, CH_4 fluxes were significantly and negatively correlated with both pH and EC in the sediment ($p < 0.01$, Table 3) when all data were pooled together. These results suggest that drainage caused a decline in both sediment EC and pH, which in turn played an important role in promoting CH_4 production and emissions from aquaculture ponds during winter.

Table 2 – Comparison of average GHG fluxes between the UDP and DP during the study period.^a

GHG ^b	Undrained pond	Drained pond	Results of RMANOVA ^c	
			F-value	p-Value
CO_2	-0.49 ± 0.09 (–0.62 to –0.31)	0.75 ± 0.12 (–0.49 to 3.65)	170.87	$<0.01^d$
CH_4	0.07 ± 0.06 (0.003 to 0.31)	0.66 ± 0.31 (0.004 to 1.77)	29.74	$<0.01^d$
N_2O	0.01 ± 0.04 (–0.27 to 0.40)	19.54 ± 2.08 (2.97 to 36.07)	164.07	$<0.01^d$

GHG: greenhouse gas.

^a Values are means \pm S.E. (range) of samples ($n = 48$).

^b CO_2 and CH_4 ($\text{mmol}/(\text{m}^2 \cdot \text{hr})$), N_2O ($\mu\text{mol}/(\text{m}^2 \cdot \text{hr})$).

^c Statistically significant differences between UDP and DP were calculated by using the repeated measures analysis of variance (RMANOVA).

^d Indicates significant difference at the 0.01 level.

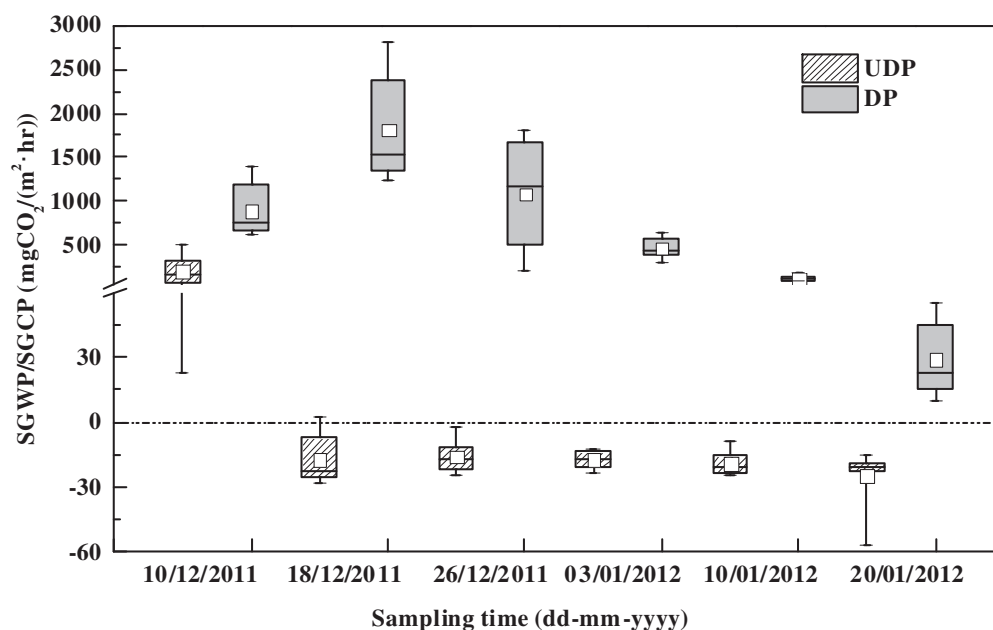


Fig. 5 – Sustained-flux global warming potential (SGWP) and sustained-flux global cooling potential (SGCP) (CO_2 -equivalents) based on CO_2 , CH_4 , and N_2O fluxes. Boxes define the 25th and 75th percentiles, whiskers define the 5th and 95th percentiles, and center lines and squares show the median and mean values, respectively.

Overall, the temporal variations in the CH_4 fluxes exhibited a similar trend for both the UDP and DP (Fig. 4b), but the dominant factor controlling CH_4 emissions was very different in each pond. Regression analysis showed that the temporal variations in the CH_4 fluxes in the UDP were mainly controlled by the EC and water SO_4^{2-} concentrations ($y = 1.696 - 0.150 \cdot \text{EC} - 0.002 \cdot \text{SO}_4^{2-}$, $F = 34.477$, $R^2 = 0.605$, $p < 0.001$), which accounted for 60.5% of CH_4 emissions; while that in DP was more dependent on temperature and pH in the sediment, as well as SO_4^{2-} concentrations in the water (Fig. 3 and Table 3).

3.3. Effect of aquaculture pond drainage on N_2O fluxes

Consistently higher N_2O emissions were observed in the DP than in the UDP during winter (Fig. 4c), indicating that drainage could also significantly increase N_2O release from aquaculture ponds ($p < 0.01$, Table 2). The difference in N_2O fluxes was mainly attributed to the change in sediment redox

status. As already discussed, a higher water depth in the UDP limits diffusion of atmospheric oxygen into the sediment, which favors the development of anaerobic conditions (Fig. 3d). This may induce denitrification in pond sediments, with much of the N_2O produced during this process being further reduced to N_2 by denitrifiers before it escapes from the sediment (Davidson et al., 2000; Hu et al., 2012; Peyron et al., 2016). As a result, net N_2O emissions in the UDP decreased significantly. On the other hand, significantly lower water depth in the DP facilitated the penetration of oxygen into the sediment (Fig. 3d), thereby stimulating microbial activity and nitrogen mineralization (Regina et al., 1996; Dinsmore et al., 2009). With a more aerobic environment, N_2O , being an intermediate product of denitrification, could be released to the atmosphere in a greater amount without further reduction over the observation period. The negative correlation between N_2O fluxes and water depth, as well as the positive correlation between the N_2O fluxes and E_h (Table 3) lend further support to our interpretation.

Table 3 – Pearson correlation coefficients between the greenhouse gas fluxes and environmental parameters.

Environmental parameters	UDP			DP			All data		
	CO_2	CH_4	N_2O	CO_2	CH_4	N_2O	CO_2	CH_4	N_2O
Water depth	NS	0.354*	0.673*	NS	0.306*	NS	-0.555**	-0.356**	-0.648**
Temperature	NS	NS	NS	0.585**	0.256*	0.301*	0.607**	0.271**	0.432**
EC	NS	-0.752**	-0.537**	NS	NS	NS	-0.315**	-0.259**	-0.274**
pH	NS	-0.610**	-0.529**	NS	-0.309**	NS	-0.574**	-0.387**	-0.671**
E_h	NS	0.613**	0.554**	NS	0.293**	NS	0.578**	0.391**	0.676**
SO_4^{2-}	NS	-0.768**	-0.526**	NS	-0.481*	NS	NS	-0.790**	-0.738**
Chl- <i>a</i>	0.186*	-0.547**	-0.653**	NS	NS	NS	-0.586**	NS	NS

NS: not significant. The symbols * and ** indicate significant correlations at the 0.05 and 0.01 levels, respectively, ($n = 48$).

UDP: undrained pond; DP: drained pond.

Another important way by which drainage can influence N_2O fluxes is through altering sediment salinity, pH, and temperature. In the present study, significant differences in sediment temperature, pH, and salinity were observed between the UDP and DP over the observation period (Table 1). Meanwhile, N_2O fluxes were positively correlated with sediment temperature, and negatively correlated with pH and EC (Table 3). These results suggest that the positive impact of drainage on N_2O emissions was related to the induced lower salinity, neutral pH, and higher sediment temperature.

3.4. Overall contribution of drained aquaculture ponds to climate change

China has been responsible for the majority of growth in fishery product supply, particularly from aquaculture ponds (FAO, 2014). Statistics show that China contains about 53% of the world's aquaculture ponds (Verdegem and Bosma, 2009), and total pond area is increasing rapidly (FAO, 2014). Considering the rapid growth of the aquaculture industry, it is important to improve the accuracy of the GHG emissions inventory in China, particularly in this sector, by quantifying the effects of different management practices on GHG fluxes from aquaculture ponds. The results of this study showed that drainage significantly increased GHG emissions from aquaculture ponds during winter in the coastal zone of southeast China. Assuming that the results of this study are representative of all aquaculture ponds in China (58,579 km^2) and that they all practice drainage from December to March, the GWPs (CO_2 equivalent units) would be 0.17 Tg CO_2 -eq for UDPs and 5.24 Tg CO_2 -eq for DPs over a 100-year timeframe. This result indicates that aquaculture pond drainage in China makes a substantial contribution to global warming. Our results imply that maintaining a relatively high water depth would be an effective strategy for reducing GHG emissions from aquaculture ponds during winter and mitigating future climate change. However, since drainage is often necessary for exporting aquaculture effluent and avoiding pond eutrophication during the non-culture period after harvest (Hu et al., 2016), developing a practical and effective way to reduce GHG emissions during the non-culture period is a top priority for the near future. We recognize that our data were from a single site at the Min River estuary and might not fully represent the magnitude of pond GHG fluxes across all coastal regions in China. To accurately estimate the effects of drainage on GHG emissions from aquaculture ponds over a broader spatial scale, further studies are required to characterize GHG emissions from ponds located in different latitudinal and climatic zones, and under different levels of management inputs.

4. Conclusions

In this study, we quantified GHG fluxes during winter in one drained and one undrained aquaculture pond from the Min River estuary of southeast China. Our results show consistent uptake and release of CO_2 in the undrained and drained ponds, respectively, with the drained pond representing a CH_4 and N_2O emissions hot spot. Furthermore, based on a new

SGWP/SGCP model, the GWP over a 100-year period in the drained pond was significantly higher than it was in the undrained pond. This finding indicates that drainage might considerably increase the contribution to global warming by aquaculture ponds in the coastal zone. Given that the drained aquaculture ponds play a significant role in increasing the GHG radiative forcing of the climate, there is a need to develop better management strategies to achieve a balance between climate change mitigation and eutrophication amelioration.

Acknowledgments

This work was supported by the National Science Foundation of China (Nos. 41671088 and 41371127), the Program for Innovative Research Team of Fujian Normal University (No. IRTL1205), the Natural Science Foundation of Fujian Province, China (No. 2014J05046), the Study-Aboard Grant Project for Graduates of the School of Geographical Sciences, (No. GY201601), and the Graduated Student Science and Technology Innovation Project of the School of Geographical Science, Fujian Normal University (No. GY201601). We sincerely thank the reviewers and editor for their valuable comments.

REFERENCES

- Avnimelech, Y., Ritvo, G., 2003. Shrimp and fish pond soils: processes and management. *Aquaculture* 220, 549–567.
- Bastviken, D., Cole, J.J., Pace, M.L., Van de Bogert, M.C., 2008. Fates of methane from different lake habitats: connecting whole-lake budgets and CH_4 emissions. *J. Geophys. Res.* 113 (G2), 1–13.
- Bastviken, D., Santoro, A.L., Marotta, H., Pinho, L.Q., Calheiros, D.F., Crill, P., Enrich-Prast, A., 2010. Methane emissions from Pantanal, South America, during the low water season: toward more comprehensive sampling. *Environ. Sci. Technol.* 44 (14), 5450–5455.
- Chambers, L.G., Osborne, T.Z., Reddy, K.R., 2013. Effect of salinity-altering pulsing events on soil organic carbon loss along an intertidal wetland gradient: a laboratory experiment. *Biogeochemistry* 115, 363–383.
- Chen, G.C., Tam, N.F.Y., Ye, Y., 2010. Summer fluxes of atmospheric greenhouse gases N_2O , CH_4 and CO_2 from mangrove soil in South China. *Sci. Total Environ.* 408, 2761–2767.
- Chen, Y., Dong, S.L., Wang, Z.N., Wang, F., Gao, Q.F., Tian, X.L., Xiong, Y.H., 2015. Variations in CO_2 fluxes from grass carp *Ctenopharyngodon idella* aquaculture polyculture ponds. *Aquacult. Environ. Interact.* 8, 31–40.
- Chen, Y., Dong, S.L., Wang, F., Gao, Q.F., Tian, X.L., 2016. Carbon dioxide and methane fluxes from feeding and no-feeding mariculture ponds. *Environ. Pollut.* 212, 489–497.
- Chimner, R.A., Cooper, D.J., 2003. Influence of water table levels on CO_2 emissions in a Colorado subalpine fen: an in situ microcosm study. *Soil Biol. Biochem.* 35 (3), 345–351.
- Clough, T.J., Buckthought, L.E., Casciotti, K.L., Kelliher, F.M., Jones, P.K., 2011. Nitrous oxide dynamics in a braided river system, New Zealand. *J. Environ. Qual.* 40 (5), 1532–1541.
- Datta, A., Nayak, D.R., Sinhababu, D.P., Adhya, T.K., 2009. Methane and nitrous oxide emissions from an integrated rainfed rice-fish farming system of Eastern India. *Agric. Ecosyst. Environ.* 129, 228–237.
- Davidson, E.A., Keller, M., Erickson, H.E., Verchot, L.V., Veldkamp, E., 2000. Testing a conceptual model of soil emissions of nitrous and nitric oxides: using two functions based on soil

- nitrogen availability and soil water content, the hole-in-the-pipe model characterizes a large fraction of the observed variation of nitric oxide and nitrous oxide emissions from soils. *Bioscience* 50, 667–680.
- Diem, T., Koch, S., Schwarzenbach, S., Wehrli, B., Schubert, C.J., 2012. Greenhouse gas emissions (CO_2 , CH_4 , and N_2O) from several perialpine and alpine hydropower reservoirs by diffusion and loss in turbines. *Aquat. Sci.* 74, 619–635.
- Dinsmore, K.J., Skiba, U.M., Billett, M.F., Rees, R.M., 2009. Effect of water table on greenhouse gas emissions from peatland mesocosms. *Plant Soil* 318, 229–242.
- FAO, 2012. The State of World Fisheries and Aquaculture 2012. Food and Agriculture Organization of the United Nations, Fisheries and Aquaculture Department, Rome, Italy.
- FAO, 2014. The State of World Fisheries and Aquaculture, 2014. Food and Agricultural Organization of the United Nations, Rome, Italy.
- Gleason, R.A., Tangen, B.A., Browne, B.A., Euliss Jr., N.H., 2009. Greenhouse gas flux from cropland and restored wetlands in the prairie pothole region. *Soil Biol. Biochem.* 41, 2501–2507.
- Gu, B.H., Schelske, C.L., Coveney, M.F., 2011. Low carbon dioxide partial pressure in a productive subtropical lake. *Aquat. Sci.* 73, 317–330.
- Haque, M.M., Biswas, J.C., Kim, S.Y., Kim, P.J., 2016. Suppressing methane emission and global warming potential from rice fields through intermittent drainage and green biomass amendment. *Soil Use Manag.* 2015 (32), 72–79.
- Hatala, J.A., Detto, M., Sonnentag, O., Deverel, S.J., Verfaillie, J., Baldocchi, D.D., 2012. Greenhouse gas (CO_2 , CH_4 , H_2O) fluxes from drained and flooded agricultural peatlands in the Sacramento-San Joaquin Delta. *Agric. Ecosyst. Environ.* 150, 1–18.
- Herbeck, L.S., Unger, D., Wu, Y., Jennerjahn, T.C., 2013. Effluent, nutrient and organic matter export from shrimp and fish ponds causing eutrophication in coastal and back-reef waters of NE Hainan, tropical China. *Cont. Shelf Res.* 57, 92–104.
- Hu, Z., Lee, J.W., Chandran, K., Kim, S., Khanal, S.K., 2012. Nitrous oxide (N_2O) emission from aquaculture: a review. *Environ. Sci. Technol.* 46 (12), 6470–6480.
- Hu, Z., Lee, J.W., Chandran, K., Kim, S., Sharma, K., Khanal, S.K., 2014. Influence of carbohydrate addition on nitrogen transformations and greenhouse gas emissions of intensive aquaculture system. *Sci. Total Environ.* 470–471, 193–200.
- Hu, Z.Q., Wu, S., Ji, C., Zou, J.W., Zhou, Q.S., Liu, S.W., 2016. A comparison of methane emissions following rice paddies conversion to crab-fish farming wetlands in southeast China. *Environ. Sci. Pollut. Res.* 23 (2), 1505–1515.
- Maberly, S.C., 1996. Diel, episodic and seasonal changes in pH and concentrations of inorganic carbon in a productive lake. *Freshw. Biol.* 35, 579–598.
- Molnar, N., Welsh, D.T., Marchand, C., Deborde, J., Meziane, T., 2013. Impacts of shrimp farm effluent on water quality, benthic metabolism and N-dynamics in a mangrove forest (New Caledonia). *Estuar. Coast. Shelf Sci.* 117, 12–21.
- Neubauer, S.C., Megonigal, J.P., 2015. Moving beyond global warming potentials to quantify the climatic role of ecosystems. *Ecosystems* 18, 1000–1013.
- Pandey, A., Mai, V.T., Vu, D.Q., Bui, T.P.L., Mai, T.L.A., Jensen, L.S., de Neergaard, A., 2014. Organic matter and water management strategies to reduce methane and nitrous oxide emissions from rice paddies in Vietnam. *Agric. Ecosyst. Environ.* 196, 137–146.
- Paudel, S.R., Choi, O., Khanal, S.K., Chandran, K., Kim, S., Lee, J.W., 2015. Effects of temperature on nitrous oxide (N_2O) emission from intensive aquaculture system. *Sci. Total Environ.* 518, 16–23.
- Peyron, M., Bertora, C., Pelissetti, S., Said-Pullicino, D., Celi, L., Miniotti, E., Romani, M., Sacco, D., 2016. Greenhouse gas emissions as affected by different water management practices in temperate rice paddies. *Agric. Ecosyst. Environ.* 232, 17–28.
- Rath, K.M., Rousk, J., 2015. Salt effects on the soil microbial decomposer community and their role in organic carbon cycling: a review. *Soil Biol. Biochem.* 81, 108–123.
- Regina, K., Nykänen, H., Silvola, J., Martikainen, P.J., 1996. Fluxes of nitrous oxide from boreal peatlands as affected by peatland type, water table level and nitrification capacity. *Biogeochemistry* 35 (3), 401–418.
- Repo, M., Huttunen, J., Naumov, A., Chichulin, A., Lapshina, E., Bleuten, W., Martikainen, P., 2007. Release of CO_2 and CH_4 from small wetland lakes in western Siberia. *Tellus B* 59, 788–796.
- Schade, J.D., Bailio, J., McDowell, W.H., 2016. Greenhouse gas flux from headwater streams in New Hampshire, USA: patterns and drivers. *Limnol. Oceanogr.* 61, S165–S174.
- Stow, C.A., Walker, J.T., Cardoch, L., Spence, P., Geron, C., 2005. N_2O emissions from streams in the Neuse River watershed, North Carolina. *Environ. Sci. Technol.* 39 (18), 6999–7004.
- Su, Y.P., Ma, S., Tian, X.L., Dong, S.L., 2009. An experimental study on nitrogen, phosphorus and carbon budgets in intensive pond of shrimp *Fenneropenaeus chinensis*. *South China. Fish. Sci.* 5 (6), 54–58.
- Sun, Z.G., Wang, L.L., Tian, H.Q., Jiang, H.H., Mou, X.J., Sun, W.L., 2013. Fluxes of nitrous oxide and methane in different coastal Suaeda salsa marshes of the Yellow River estuary, China. *Chemosphere* 90 (2), 856–865.
- Tam, F.Y., Wong, Y.S., 1998. Variations of soil nutrient and organic matter content in a subtropical mangrove ecosystem. *Water Air Soil Pollut.* 103 (1), 245–261.
- Tangen, B.A., Finocchiaro, R.G., Gleason, R.A., Dahl, C.F., 2016. Greenhouse gas fluxes of a shallow lake in south-central North Dakota, USA. *Wetlands* 36, 779–787.
- The Fishery Bureau, Ministry of Agriculture of PRC, 2014. Statistical Overview of National Fishery. Chinese Agriculture Press, Beijing.
- Tong, C., Huang, J.F., Hu, Z.Q., Jin, Y.F., 2013. Diurnal variations of carbon dioxide, methane, and nitrous oxide vertical fluxes in a subtropical estuarine marsh on neap and spring tide days. *Estuar. Coasts* 36 (3), 633–642.
- Verdegem, M.C.J., Bosma, R.H., 2009. Water withdrawal for brackish and inland aquaculture, and options to produce more fish in ponds with present water use. *Water Policy* 11 (Suppl. 1), 52–68.
- Wang, F.S., Cao, M., Wang, B.L., Fu, J.N., Luo, W.Y., Ma, J., 2015. Seasonal variation of CO_2 diffusion flux from a large subtropical reservoir in East China. *Atmos. Environ.* 103, 129–137.
- Weston, N.B., Dixon, R.E., Joye, S.B., 2006. Ramifications of increased salinity in tidal freshwater sediments: geochemistry and microbial pathways of organic matter mineralization. *J. Geophys. Res. Biogeosci.* 111 (G1), 689–699.
- Williams, J., Crutzen, P.J., 2010. Nitrous oxide from aquaculture. *Nat. Geosci.* 3, 143.
- Witte, S., Giani, L., 2016. Greenhouse gas emission and balance of marshes at the southern north sea coast. *Wetlands* 36, 121–132.
- Yagi, K., Tsuruta, H., Kanda, K., Minami, K., 1996. Effect of water management on methane emission from a Japanese rice paddy field: automated methane monitoring. *Glob. Biogeochem. Cycles* 10, 255–267.
- Yang, J.S., Liu, J.S., Hu, X.J., Li, X.X., Wang, Y., Li, H.Y., 2013. Effect of water table level on CO_2 , CH_4 and N_2O emissions in a freshwater marsh of Northeast China. *Soil Biol. Biochem.* 61, 52–60.
- Yang, H., Andersen, T., Dörsch, P., Tominaga, K., Thrane, J.-E., Hessen, D.O., 2015. Greenhouse gas metabolism in Nordic boreal lakes. *Biogeochemistry* 126 (1–2), 211–225.

- Zeng, C.S., Wang, W.Q., Tong, C., 2008. Effects of different exogenous electron acceptors and salt import on methane production potential of estuarine marsh soil. *Geogr. Res.* 27, 1321–1330.
- Zeng, Q.F., Gu, X.H., Chen, X., Mao, Z.G., 2013. The impact of Chinese mitten crab culture on water quality, sediment and the pelagic and macrobenthic community in the reclamation area of Guchenghu Lake. *Fish. Sci.* 79, 689–697.
- Zhao, Y., Wu, B.F., Zeng, Y., 2013. Spatial and temporal patterns of greenhouse gas emissions from Three Gorges Reservoir of China. *Biogeosciences* 10, 1219–1230.